Journal of Sound and Vibration (2001) **246**(5), 757–775
doi:10.1006/jsvi.2000.3450, available online at http://www.idealibrary.com on IDEAL®

THE DYNAMIC RESPONSE OF A ROTATING SHAFT SUBJECT TO AN AXIALLY MOVING AND ROTATING LOAD

R. KATZ†

The University of Michigan, Ann Arbor. E-mail: reuven@engin.umich.edu

(*Received* 2 *March* 2000, *and in final form* 13 *September* 2000)

The dynamic response of a rotating shaft subject to an axially, constant-velocity, moving and rotating load is investigated. The dynamic behaviour of future, high-speed linear bearings is studied. Shafts used in linear bearing applications are typically slender. Therefore, Rayleigh beam theory is used to model the rotating shaft. Modal analysis and integral transformation methods are employed to develop analytical expressions for the transient response of a shaft with simply supported boundary conditions. Numerical results are presented, discussed and compared with some available solutions. As shown in the paper, by changing model parameters, it is possible to describe dynamic behaviour of different types of linear bearings and other mechanical elements.

1. INTRODUCTION

The problem of a rotating shaft subject to an axially moving load was first introduced in reference [1]. It is a combined problem using methods from the field of rotor dynamics [2, 3] and from studies of structures subject to moving loads [4]. The original concern about the problem was related to the study of future high-speed machining operations. Since then, several papers have been published studying various aspects of the basic problem of a rotating shaft subject to moving load. Following the first paper, the study in reference [15] presented a generalized modal analysis method and the Galerkin method which were used to investigate the Rayleigh and Timosenko beam models of the shaft. Argento and Scott [6] have studied the problem of accelerating distributed surface load and in a later paper [7] they have extended this study using the Galerkin method to find the response of various types of load velocity profiles and shaft boundary conditions. Huang and Chen [8] studied the response of a spinning orthotropic beam subjected to a moving harmonic load using a Euler–Bernoulli model in a rotating system of co-ordinates. Huang and Hsu [9] have investigated the resonant phenomena of a rotating cylindrical shell subjected to a harmonic moving load. Zu and Han [10] have solved analytically the challenging problem of a spinning Timoshenko beam subject to a moving load with general boundary conditions. In a chapter about distributed parameter rotor-bearing systems, Lee [11] describes in detail the use of a modal analysis method for analyzing rotors and includes the case of moving load problem. Lee [12] investigated the problem of an axial load acting

†The author is Associate Research Scientist and Chief Engineer at the Center for Reconfigurable Machining Systems.

0022-460X/01/400757 + 19 $35.00/0

on the shaft in addition to the moving load. Most researchers who have studied the problem have shown great interest in the analytical problem and in the methods of solution, although possible applications of the study were hardly ever mentioned.

The study in this paper has two goals. The first is to study the dynamic response of a rotating shaft subject to moving and rotating loads. The second goal is to show that the model may describe design problems related to future high-speed moving machine elements and especially some linear bearing elements. There is an attempt to address both issues, to present an analytical solution of a novel problem in dynamics and to search for a new field of future applications where this solution may be used. The paper presents general analytical expressions for the dynamic deflections of a rotating shaft subject to axially moving and rotating loads. This type of moving load application has not been studied previously for either stationary or rotating shafts. As shown in the paper, the relations between the axial and the rotational speeds of the load and the load speed parameter α, affect the dynamic deflections of the shaft.

In the design of modern machines there is a continuous trend to reduce the size or weight of the parts, to increase relative velocities and accelerations between moving parts and to increase accuracy while operating in a noisy environment. Those generic requirements force designers to choose and to calculate carefully each machine element. The above-mentioned requirements will become even harder in the future due to growing competition in the markets. The examples described in the paper are from the field of linear motion elements, which are widely used in the design of machine tools, robotics, electro-mechanical devices and memory drives. The linear motion elements are designed and built as high precision devices. Those devices should be accurate under static or dynamic conditions. Some manufacturer's catalogues suggest a guide for correct design. For example, in order to choose a "rotary spline screw", the designer should validate that the applied rotational speed of the machine will be lower than 80% of the fundamental natural frequency. As can be seen, the manufacturer suggests using the device as a sub-critical system. Once the rotational and axial speeds increase, one should calculate the system more precisely. The rotating shaft, which is subjected to a moving and rotating load, is expected to have deflection amplification which indicates inaccuracy of the bearing. When accuracy is measured in micro-metres and the relative velocity of the applied loads is significant, dynamic insight into the problem is required.

2. EQUATIONS OF MOTION

The general model of a rotating beam subject to a moving load was derived in references [1] and [13] and will not be repeated here. The Rayleigh beam model is used to describe the problem, since the shafts used in linear bearing designs are typically slender. The model includes the gyroscopic model terms and the moment terms due to the inertia of rotation of cross-sections. Unlike in the Timoshenko beam model, here the shear deformation terms are neglected. Some additional simplifying assumptions are used to analyze the transient response of a shaft subject to an axially moving and rotating load, as shown in Figure 1. The study is limited to the case of a uniform and balanced shaft with a circular cross-section, which is simply supported and rotating at constant speed (ω). It is further assumed that the shaft is not subjected to axial forces. The applied force $P(z, t)$ is of constant magnitude, and moves with a constant axial velocity (v) along the shaft axis OX_1. The load also rotates at a constant velocity $p(t)$ that may be positive i.e., in the same direction as the rotation of the shaft, or negative in a direction which is opposite to the shaft direction of rotation, as shown in Figure 2. The load remains parallel to the OX_1X_2 plane.

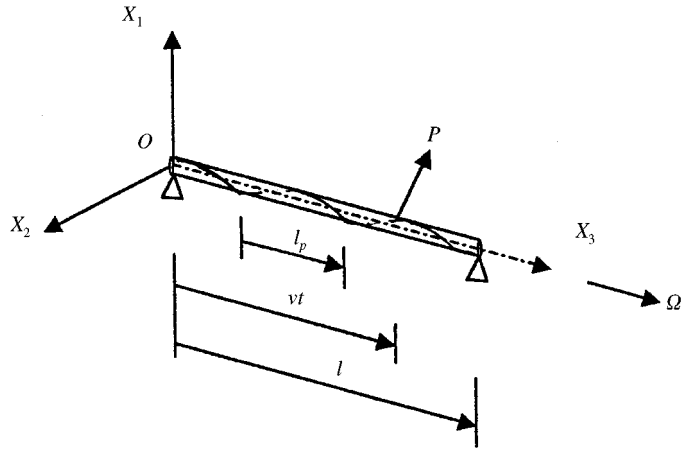

Figure 1. Moving and rotating load.

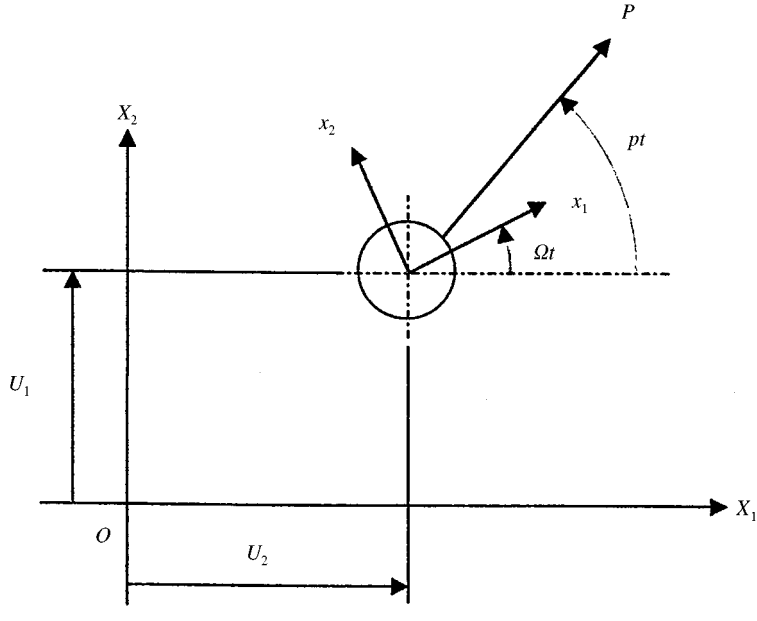

Figure 2. System of co-ordinates.

Using complex notation, the equation of motion is

$$EI\frac{\partial^4 U}{\partial z^4} + \rho A\frac{\partial^2 U}{\partial t^2} - \rho I\left[\frac{\partial^4 U}{\partial z^2 \partial t^2} - \mathrm{i}2\Omega\frac{\partial^3 U}{\partial z^2 \partial t}\right] = P(z, t), \tag{1}$$

where the load and the deflection terms are

$$P(z, t) = P\delta(z - vt)\mathrm{e}^{\mathrm{i}pt} \tag{2}$$

$$U = U_1 + \mathrm{i}U_2 \tag{3}$$

Equation (1) is equivalent to a set of two coupled equations in the OX_1X_3 and OX_2X_3 directions. The coupling is due to the gyroscopic term. The well-known boundary conditions and initial conditions for a simply supported beam are used here.

3. RESPONSE TO AXIALLY MOVING AND ROTATING LOAD

In this Section the response to an axially moving and rotating load is presented for the Rayleigh beam model. The transient response for the time period $0 < t < (l/v)$ is considered, which is the time required for the load to traverse the shaft. The response of the rotating shaft is presented in an inertial system of co-ordinates. In some literature the finite integral transformation method was used as a convenient method for solving the Rayleigh beam model [4]. The method of modal analysis is introduced here in order to provide a better physical insight into the problem. The method of solution used in this paper is hybrid. It applies both modal analysis and finite integral transformation methods to obtain analytical expressions for the deflections under the moving load. A more general treatment of modal analysis for analyzing the response of rotating shafts subject to moving loads may be found in reference [1].

In order to help the reader a brief reminder of the method of the solution of the homogeneous equation shown in references [1] and [11] is repeated here.

Consider the homogeneous part of equation (1) and assume the solution is

$$U(z, t) = \sum_{n=1}^{\infty} \phi_n(z)\eta_n(t) = \sum_{n=1}^{\infty} \bar{u}_n \exp\left(\mathrm{i}\sqrt{\tau_n}\,\frac{z}{l}\right)\exp(\mathrm{i}\omega_n t), \tag{4}$$

where $\bar{u}_n$ is the complex amplitude, τ_n characterizes the mode shapes and ω_n are the natural frequencies. Substituting equation (4) into the homogeneous part of equation (1) gives

$$EI\phi_n'''' - 2\rho A r_0^2 \Omega\omega_n\phi_n'' + \rho A\omega_n^2(-\phi_n + r_0^2\phi_n'') = 0 \tag{5}$$

or

$$(EI/l^4)\tau_n^2 + (\rho A r_0^2/l^2)(\omega_n^2 - 2\Omega\omega_n)\tau_n - \rho A\omega_n^2 = 0. \tag{6}$$

The solution of equation (6) leads to the general equation of the eigenvalues. Here, for a simply supported shaft, one may use without loss of generality the simple form eigenfunction,

$$\phi_n(z) = \sin\frac{n\pi}{l}\,z \tag{7}$$

The corresponding natural frequencies are determined from equations (5) and (7) and are

$$(1 + \beta_n^2)\omega_n^2 - 2\Omega\beta_n^2\omega_n - \omega_{nEB}^2 = 0, \tag{8}$$

where the Rayleigh coefficient and the Euler–Bernoulli natural frequency of the shaft are given by

$$\beta_n = \left(\frac{n\pi r_0}{l}\right)^2, \qquad \omega_{nEB}^2 = \left(\frac{n\pi}{l}\right)^4\left(\frac{EI}{\rho A}\right). \tag{9}$$

Solving equation (8) gives

$$\omega_{n_{1,2}} = [\Omega\beta_n^2 \pm \sqrt{\Omega^2\beta_n^4 + (1+\beta_n^2)\omega_{nEB}^2}]/(1+\beta_n^2). \tag{10}$$

Here it is important to note that two natural frequencies exist, one (ω_{n1}) always being positive (forward precession) and the other (ω_{n2}) negative (backward precession), corresponding to a single eigenfunction. Boundary conditions other than those simply supported should be treated differently [5].

Multiplying equation (5) by ϕ_m and integrating over the length of the shaft, using the boundary conditions and integrating by parts results in

$$-\omega_n^2 H_{nm} + \omega_n L_{nm} + K_{nm} = 0, \tag{11}$$

where

$$H_{nm} = \frac{\rho Al}{2}(1+\beta_n^2)\delta_{nm}, \qquad L_{nm} = \rho Al\Omega\beta_n^2\delta_{nm}, \tag{12, 13}$$

$$K_{nm} = \frac{EIl}{2}\left(\frac{n\pi}{l}\right)^4\delta_{nm}. \tag{14}$$

δ_{nm} is the Kronecker delta function. In equation (11), the case $m \neq n$ becomes a trivial one. For $m = n$, equation (11) becomes

$$-\omega_n^2 H_{nn} + \omega_n L_{nn} + K_{nn} = 0. \tag{15}$$

Equation (15) also implicitly indicates that two natural frequencies exist corresponding to a single mode ω_{n1} and ω_{n2}. The orthogonality condition for the eigenvalues are stated in equation (11) and in the following relations:

$$(\omega_{n_1} + \omega_{n_2})H_{nn} = L_{nn}, \qquad -\omega_{n_1}\omega_{n_2}H_{nn} = K_{nn} \tag{16}$$

3.1. THE GENERAL CASE $p \neq \Omega$

The analytical expression that describes the transient response of the rotating shaft subject to an axially moving and rotating load, is one goal of our study. Therefore, the next step is to solve the non-homogeneous equation (1). Introducing equation (11) in equation (6), multiplying by ϕ_m, integrating over the length of the shaft, and using the relations in equation (16) gives

$$\ddot{\eta}_n - \mathrm{i}(\omega_{n_1} + \omega_{n_2})\dot{\eta}_n - \omega_{n_1}\omega_{n_2}\eta_n = \frac{1}{H_{nn}}\int_0^1 P(z,t)\phi_n \,\mathrm{d}z. \tag{17}$$

Equation (17) describes an infinite set of ordinary differential equations. Upon solving for $\eta_n(t)$, the complex generalized co-ordinate, the total deflection, given in a complex form, is obtained by using equation (4). Considering a moving load of the form of equation (2), equation (17) gives

$$\ddot{\eta}_n - \mathrm{i}(\omega_{n_1} + \omega_{n_2})\dot{\eta}_n - \omega_{n_1}\omega_{n_2}\eta_n = \frac{2P\mathrm{e}^{\mathrm{i}pt}}{\rho Al(1+\beta_n^2)}\sin\left(\frac{n\pi v}{l}\right)t. \tag{18}$$

Applying the Laplace transformation method equation (18) can be solved:

$$\bar{\eta}_n(s) = \frac{2P}{\rho A l} \frac{\theta_n}{(1+\beta_n^2)} \frac{1}{(s - \mathrm{i}\omega_{n_1})(s - \mathrm{i}\omega_{n_2})(s - \mathrm{i}r_1)(s + \mathrm{i}r_2)}, \tag{19}$$

where

$$\theta_n = \frac{n\pi v}{l}, \qquad r_1 = \theta_n + p, \qquad r_2 = \theta_n - p. \tag{20}$$

It is important to notice that r_1 and r_2 are frequencies which describe the moving and rotating load. Each of them is a combination of θ_n which is the frequency that represents the axial motion of the load, and p which is the angular frequency of the load rotation. The frequency p is positive when the load is rotating in the same direction as the shaft.

The expression for η_n can be written in the form

$$\begin{aligned}\bar{\eta}_n(s) = \frac{2P}{\rho A l} \frac{\theta_n}{1+\beta_n^2} \Bigg\{ & \frac{\mathrm{i}}{(\omega_{n_1} - \omega_{n_2})(\omega_{n_1} - r_1)(\omega_{n_1} + r_2)} \frac{1}{(s - \mathrm{i}\omega_{n_1})} \\ & - \frac{\mathrm{i}}{(\omega_{n_1} - \omega_{n_2})(\omega_{n_2} - r_1)(\omega_{n_2} + r_2)} \frac{1}{(s - \mathrm{i}\omega_{n_2})} + \frac{\mathrm{i}}{(\omega_{n_1} - r_1)(\omega_{n_2} - r_1)(r_1 + r_2)} \\ & \times \frac{1}{s - \mathrm{i}r_1} - \frac{\mathrm{i}}{(\omega_{n_1} + r_2)(\omega_{n_2} + r_2)(r_1 + r_2)} \frac{1}{(s + \mathrm{i}r_2)} \Bigg\}. \end{aligned} \tag{21}$$

The inverse Laplace transform, upon noting that the poles are simple, and using the residue theorem, is found to be

$$\begin{aligned}\bar{\eta}_n(t) = \frac{2P}{\rho A l} & \frac{\mathrm{i}\theta_n}{(\omega_{n_1} - \omega_{n_2})(r_1 + r_2)(\omega_{n_1} - r_1)(\omega_{n_1} + r_2)(\omega_{n_2} - r_1)(\omega_{n_2} + r_2)} \\ & \times \{(\omega_{n_2} - r_1)(\omega_{n_2} + r_2)(r_1 + r_2)\mathrm{e}^{\mathrm{i}\omega_{n_1}t} - (\omega_{n_1} - r_1)(\omega_{n_1} + r_2)(r_1 + r_2)\mathrm{e}^{\mathrm{i}\omega_{n_2}t} \\ & + (\omega_{n_1} - \omega_{n_2})(\omega_{n_1} + r_2)(\omega_{n_2} + r_2)\mathrm{e}^{\mathrm{i}r_1 t} - (\omega_{n_1} - \omega_{n_2})(\omega_{n_1} - r_1)(\omega_{n_2} - r_1)\mathrm{e}^{-\mathrm{i}r_2 t}\}. \end{aligned} \tag{22}$$

The response, given in complex form, is

$$U(z, t) = \sum_{n=1}^{\infty} \eta_n(t) \sin(n\pi t/l). \tag{23}$$

To obtain the response in the OX_1 and OX_2 directions (U_1 and U_2 respectively) the following transformations are used:

$$\eta_{n_1} = \tfrac{1}{2}(\eta_n + \eta_n^*), \qquad \eta_{n_2} = \tfrac{1}{2\mathrm{i}}(\eta_n - \eta_n^*), \tag{24}$$

where η_n^* is the complex conjugate of η_n.

The expressions for the deflections under the moving load are

$$U_1(z,t) = \sum_{n=1}^{\infty} \frac{2P}{\rho A l} \frac{\theta_n}{(1+\beta_n^2)}$$

$$\times \frac{1}{(\omega_{n_1}-\omega_{n_2})(r_1+r_2)(\omega_{n_1}-r_1)(\omega_{n_1}+r_2)(\omega_{n_2}-r_1)(\omega_{n_2}+r_2)}$$

$$\times \{ -(\omega_{n_2}-r_1)(\omega_{n_2}+r_2)(r_1+r_2)\sin\omega_{n_1}t + (\omega_{n_1}-r_1)(\omega_{n_1}+r_2)(r_1+r_2)\sin\omega_{n_2}t$$

$$-(\omega_{n_1}-\omega_{n_2})(\omega_{n_1}+r_2)(\omega_{n_2}+r_2)\sin r_1 t - (\omega_{n_1}-\omega_{n_2})(\omega_{n_1}-r_1)$$

$$\times (\omega_{n_2}-r_1)\sin r_2 t\} \sin\frac{n\pi}{l} z \tag{25}$$

and

$$U_2(z,t) = \sum_{n=1}^{\infty} \frac{2P}{\rho A l} \frac{\theta_n}{(1+\beta_n^2)}$$

$$\times \frac{1}{(\omega_{n_1}-\omega_{n_2})(r_1+r_2)(\omega_{n_1}-r_1)(\omega_{n_1}+r_2)(\omega_{n_2}-r_1)(\omega_{n_2}+r_2)}$$

$$\times \{(\omega_{n_2}-r_1)(\omega_{n_2}+r_2)(r_1+r_2)\cos\omega_{n_1}t - (\omega_{n_1}-r_1)(\omega_{n_1}+r_2)(r_1+r_2)\cos\omega_{n_2}t$$

$$+(\omega_{n_1}-\omega_{n_2})(\omega_{n_1}+r_2)(\omega_{n_2}+r_2)\cos r_1 t - (\omega_{n_1}-\omega_{n_2})(\omega_{n_1}-r_1)$$

$$\times (\omega_{n_2}-r_1)\cos r_2 t\} \sin\frac{n\pi}{l} z. \tag{26}$$

Equations (25) and (26) represent a general solution of the deflections of a simply supported rotating shaft due to the combined motion of a load which is rotating and axially moving at high velocities. As expected in this case, significant deflections are seen in both directions OX_1 and OX_2. Since the length of the shaft is final, it is interesting to explore the behaviour of the shaft under different parameters.

This model may be directly applied to evaluate the future high-speed rotary spline screw (RSS) that is described in Figure 3. The RSS is a machine element that has three degrees of freedom. It enables the rotation of the spline shaft on a couple of angular end bearings at (Ω) [rad/s]. The linear ball screw may perform an axial linear motion (v) (m/s) relative to the moving shaft. The load is applied to the external ring that is mounted on a radial bearing and enables rotation in the positive and negative directions (p) (rad/s) according to the design requirements. In this case the linear and rotational motions of the load are independent. The RSS is a high precision element currently used to build machine tools, robots or medical devices.

Figure 4 describes a rotating ball spline (RBS). It is a two-degree-of-freedom element where both ends of the spline are circular and enable the rotation of the spline shaft on a couple of angular end bearings at (Ω) (rad/s). The load, applied at the outer ring of the axial bearing is forced to move axially relative to the shaft while rotating with the spline shaft. Here the motion of the load as seen from the inertial system of co-ordinates is dependent on (Ω) the rotational velocity of the shaft and on (v) the axial velocity. These two

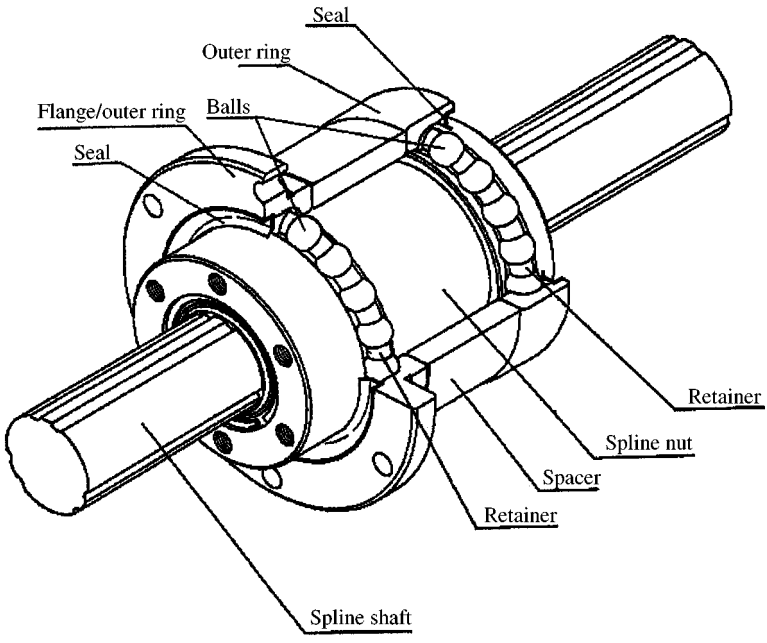

Figure 3. Rotary spline screw (RSS).

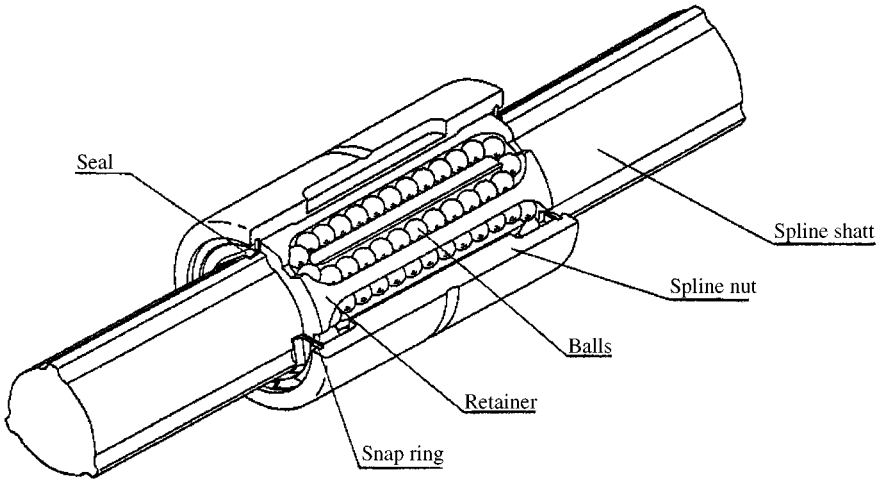

Figure 4. Rotating ball spline (RBS).

parameters determine loads' "pitch length". For constant rotational velocity of the shaft, the higher the axial velocity of the load the larger the "pitch length".

Figure 5 describes a leading screw (LS). It is a single-degree-of-freedom machine element. The load is applied to the screw externally. It moves axially and rotates at the same time according to the screw pitch equation. This machine element is widely used in many applications of machine design.

The demand for higher operational speeds and better accuracy is the natural trend of the industry, due to the competition on the market. The model presented may be useful in analyzing and achieving improved requirements for various linear motion devices.

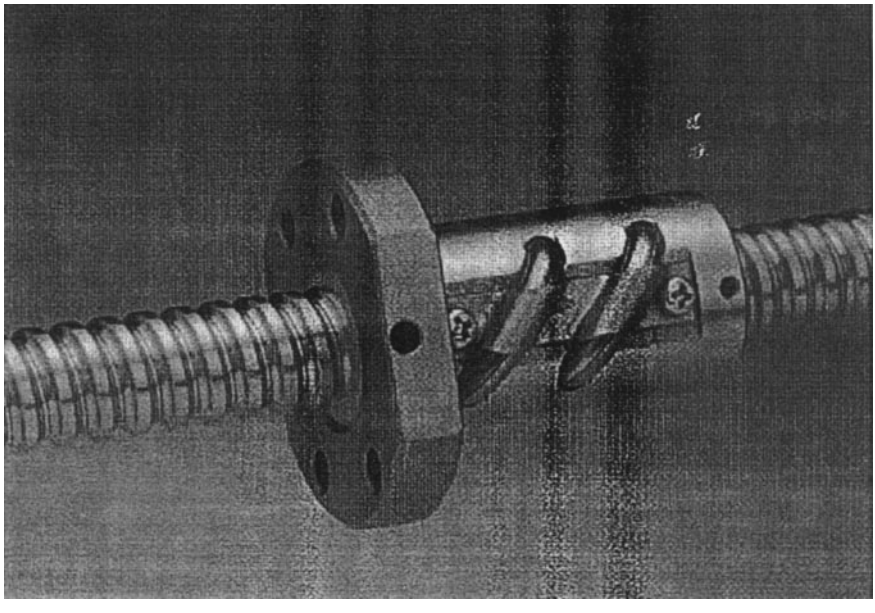

Figure 5. Leading screw (LS).

Consider next some special cases, which are derived from the general study. Some models may represent different machine elements.

3.2. ROTATING SHAFT, RESONANCE CONDITIONS ($\omega_{n_1} = -r_2$)

The natural forward and backward frequencies of the shaft are dependent on its rotational velocity (Ω), on the Rayleigh beam coefficient (β_n) and on shaft properties. There are two frequencies that describe the nature of the applied load. (θ_n) which represents its axial velocity and (p) which represents its rotation. r_1 and r_2 are two frequencies which represent the combined behaviour of the load.

As may be observed, there are four possible resonance frequencies:

$$\omega_{n1} = r_1, \qquad \omega_{n1} = -r_2, \qquad \omega_{n2} = r_1, \qquad \omega_{n2} = -r_2.$$

It is known that $|\omega_{n2}| < \omega_{n1}$ and that $|r_1| > |r_2|$.

Therefore, checking the forward precession of the shaft, the case of $\omega_{n1} = -r_2$ is more likely to occur. This case is presented here, as an example, in order to show the nature of the resonance equations. It is a case that mathematically involves a double pole solution. Only the final expressions are presented here.

$$U_1(z,t) = \sum_{n=1}^{\infty} \frac{2P}{\rho A l} \frac{\theta_n}{(1+\beta_n^2)} [-Q_1 t \cos\omega_{n_2} t + Q_2 \sin\omega_{n_2} t + Q_3 \sin r_2 t - Q_4 \sin\omega_{n_1} t] \sin\frac{n\pi}{l} z,$$

$$U_2(z,t) = \sum_{n=1}^{\infty} \frac{2P}{\rho A l} \frac{\theta_n}{(1+\beta_n^2)} [-Q_1 t \sin\omega_{n_2} t - Q_2 \cos\omega_{n_2} t + Q_3 \cos r_2 t + Q_4 \cos\omega_{n_1} t] \sin\frac{n\pi}{l} z, \tag{27}$$

where

$$Q_1 = \frac{1}{(\omega_{n_2} - \omega_{n_1})(\omega_{n_2} - r_2)}, \quad Q_2 = \frac{(2\omega_{n_2} - \omega_{n_1} + r_2)}{(\omega_{n_2} - \omega_{n_1})^2(\omega_{n_2} - r_2)^2},$$

$$Q_3 = \frac{1}{(\omega_{n_2} - r_2)^2(\omega_{n_1} + r_2)}, \quad Q_4 = \frac{1}{(\omega_{n_2} - \omega_{n_1})^2(\omega_{n_1} + r_2)}.$$

The terms $t\cos(\omega_{n2}t)$ and $t\sin(\omega_{n2}t)$ are growing linearly with time. For this study of the transient response of a high-speed load traversing a finite length shaft, the deflection of the shaft remains bounded. Similar expressions may be derived for all other resonance cases.

3.3. ROTATING SHAFT SUBJECTED TO NON-ROTATING MOVING LOAD ($p = 0$)

This is the case of a rotating shaft subject to an axially moving load. Here, since $p = 0$, $r_1 = r_2 = \theta_n$. Inserting these values into equations (25) and (26) gives the expressions developed in reference [1]. It is important to mention again that a load that is moving axially on the shaft in one inertial plane say, OX_1X_3 creates deflection not only in this plane, but also in the perpendicular direction OX_2, due to the coupling gyroscopic effect.

3.4. STATIONARY SHAFT SUBJECTED TO MOVING AND ROTATING LOAD

This is a case of a non-rotating shaft subject to an axially moving and a rotating load. By substituting $\omega_{n1} = -\omega_{n2} = \omega_n$ into equations (25) and (26), gives the expressions for shaft deflection in both directions:

$$U_1(z,t) = \sum_{n=1}^{\infty} \frac{P}{\rho Al} \frac{1}{(1+\beta_n^2)} \frac{1}{\omega_n(\omega_n^2 - r_1^2)(\omega_n^2 - r_2^2)} \{-[(\omega_n^2 - r_2^2)r_1 + (\omega_n^2 - r_1^2)r_2]$$
$$\times \sin\omega_n t + \omega_n(\omega_n^2 - r_2^2)\sin r_1 t + \omega_n(\omega_n^2 - r_1^2)\sin r_2 t\} \sin\left(\frac{n\pi}{l}\right)z, \tag{28}$$

$$U_2(z,t) = \sum_{n=1}^{\infty} \frac{P}{\rho Al} \frac{1}{(1+\beta_n^2)} \frac{1}{(\omega_n^2 - r_1^2)(\omega_n^2 - r_2^2)} \times \{(r_1 - r_2)\cos\omega_n t - \omega_n(\omega_n^2 - r_2^2)\cos r_1 t$$
$$+ (\omega_n^2 - r_1^2)\cos r_2 t\} \sin(n\pi/l)z. \tag{29}$$

Equations (28) and (29) have been also derived directly using the Euler–Bernoulli beam model for a rotating (or non-rotating) shaft using equation (30).

$$EI\frac{\partial^4 U}{\partial z^4} + \rho A\frac{\partial^2 U}{\partial t^2} = P\delta(z - vt)e^{ipt}. \tag{30}$$

Except for the term $1/(1 + \beta_n^2)$ which is related to the Rayleigh coefficient, equations (28) and (29) are identical for both cases.

Equation (30) and the solutions given in equations (28) and (29) may resemble the results of a classical study by Timoshenko which is mentioned in reference [4]. The study was related to the problem of a moving steam locomotive on a large-span railway bridge. The two-cylinder steam locomotive has driving wheels provided with unbalanced counterweights, the right hand being placed 90° against the left hand. As a result of this

unusual loading nature, the mathematical model of the bridge subjected to the moving locomotive with an unbalanced sinusoidal load is naturally close to our model. Although the mathematical model is quite close, it is describing two totally different physical phenomena.

The case of stationary shaft subjected to a moving and rotating load is an important result from the practical point of view. It enables any leading screw (LS) and a stationary rotary spline screw (RSS) to be modelled and analyzed in a simple form. For the leading screw (LS) the relation between the axial velocity (v) and its rotational velocity (p) are dependent on the screw pitch equation. For a rotary spline screw (RSS) with a stationary shaft, the axial and rotational motions of the load are independent.

3.5. STATIONARY SHAFT SUBJECTED TO AXIALLY MOVING LOAD

This case represents an axially moving load on a stationary shaft. By substituting $\omega_{n1} = -\omega_{n2} = \omega_n$ and $p = 0$ into equations (25) and (26) they converge to the well-known expressions [4]

$$U_1(z, t) = \sum_{n=1}^{\infty} \frac{2P}{\rho Al} \frac{1}{(1 + \beta_n^2)} \frac{1}{(\omega_n^2 - \theta_n^2)} \left[\sin \theta_n t - \frac{\theta_n}{\omega_n} \sin \omega_n t \right] \sin(n\pi/l)z,$$

$$U_2(z, t) = 0. \tag{31}$$

These equations may represent a load moving on any linear ball spline with a stationary, non-rotating shaft or on any other linear bearing device which is simply supported.

TABLE 1

Nominal values of the parameters in the simulation

Parameter	Value
l	1 (m)
E	206 (GPa)
ρ	7700 (Kg/m^2)
β	0·02
Ω	1·0

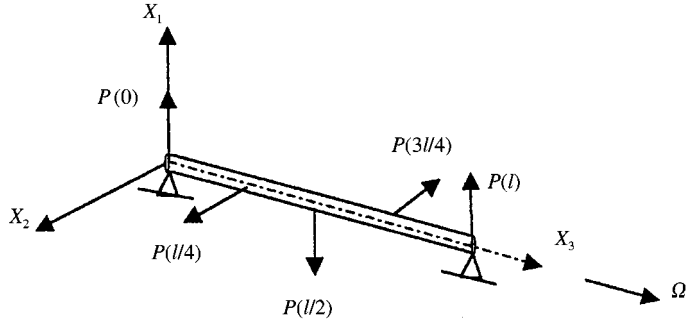

Figure 6. Directions of the rotating load along the shaft ($k_p = 1$).

4. NUMERICAL EXAMPLES AND DISCUSSION

4.1. EXAMPLE 1—DYNAMIC DEFLECTION OF A ROTATING SHAFT UNDER AN AXIALLY MOVING AND ROTATING LOAD

Future families of linear motion products will face new demands: higher speeds of motion, higher precision and reduced weight and price. The challenge of meeting these demands requires a better understanding of the problem and improved analysis tools.

The example to be studied here may represent a commercial rotating ball spline (RBS). The typical dimensions and material properties shown here can be found in a catalogue.

In the study a set of non-dimensional parameters are used. The normalized deflections under the moving load U_1/U_s and U_2/U_s are calculated along the shaft. In order to use the terminology of references [4] and [1] the value of α—the speed ratio (v/v_{cr}) is first defined. Since v_{cr} is shaft property, α defines the load velocity v. Next k_p is chosen, which represents the number of rotations that the load completes while traversing at velocity (v) along the shaft length (l). Once v and k_p are known, p the frequency of rotation of the moving load is prescribed using equation (32). In addition β is defined as the Rayleigh beam coefficient and Ω as the non-dimensional speed of the shaft. The dynamic response of a shaft subjected to a non-rotating moving load as a function of varying parameters has been investigated in previous papers [1, 5]. In this paper some special phenomena which are related to the rotation of the moving load traversing a rotating shaft are to be investigated.

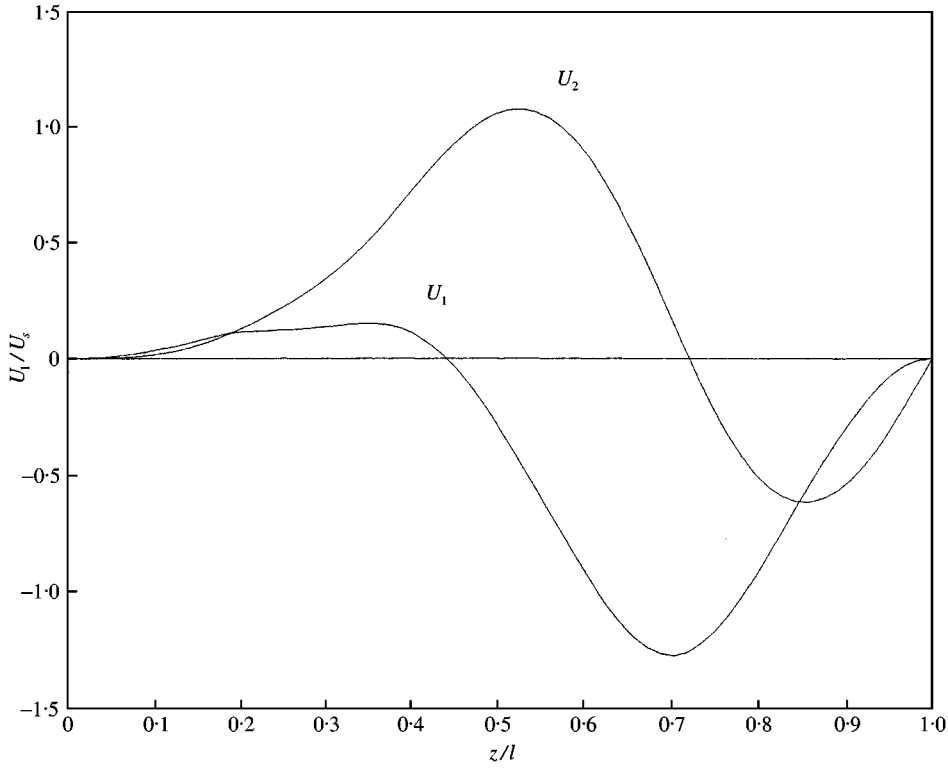

Figure 7. Dynamic deflections of a rotating shaft under moving and rotating load ($k_p = 1$, $\alpha = 0{\cdot}5$).

The rotational velocity of the load is related to the linear velocity of the load through the pitch equation

$$p = k_p(2\pi v/l), \tag{32}$$

$k_p = l/l_p$ and is the ratio between the length of the shaft and the "load pitch length" (l_p) as shown in Figure 1.

In order to get results that are comparable, any single rotation of the load relative to the inertial set of co-ordinates is divided into four quarters.

The parameters used to investigate the problem are given in Table 1.

The numerical convergence of the series is very good, being proportional to $1/n^4$. For all cases presented here $n = 10$ was used and proved sufficient.

In order to get some insight into the problem consider $k_p = 1$ which means that the load will complete one full rotation while traversing the shaft given $\alpha = 0{\cdot}5$. The position of the load at the end of each quarter of the shaft is described in Figure 6. The results of the normalized non-dimensional deflections of the shaft under the moving load are shown in Figure 7. Observing Figures 6 and 7, one may see that the load is directed in the positive direction of X_1 at both ends of the shaft and is directed in the negative direction of X_1 at the middle of the shaft. The load is directed towards the positive direction of X_2 in the first quarter of the shaft and towards the negative direction in the third quarter. This explains why the maximal deflection U_2/U_s of the shaft is built up first in the positive direction of X_2 and changes signs towards its end. It also becomes clear why the deflection U_1/U_s achieves

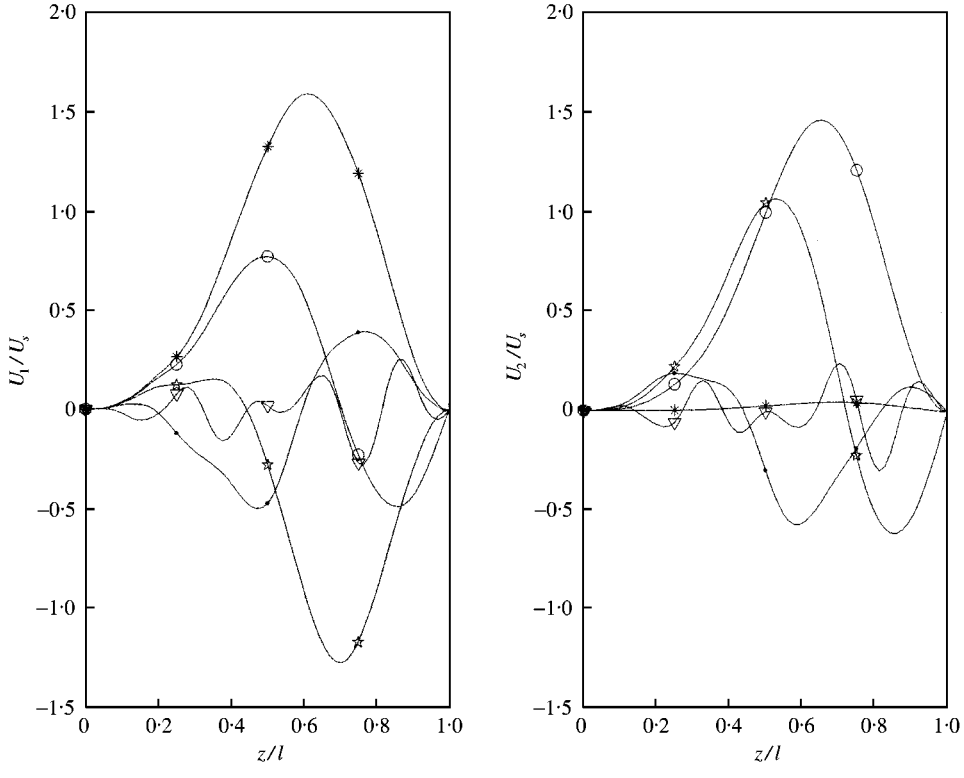

Figure 8. Dynamic deflections of a rotating shaft under moving and rotating load ($\alpha = 0{\cdot}5$; ∗, $k_p = 0{\cdot}01$; ○, $k_p = 0{\cdot}5$; ☆, $k_p = 1$; ●, $k_p = 2$; ▽, $k_p = 5$).

its maximum in the negative direction of X_1 and why it lags behind the maximal peak of U_2/U_s. Both maximal peaks of U_1/U_s and U_2/U_s are greater than one, which means that there is some amplification of the shaft deflection relative to the static deflection.

Figure 8 shows shaft deflections U_1/U_s and U_2/U_s for $\alpha = 0{\cdot}5$ and five different values of k_p. The value $k_p = 0{\cdot}01$ is describing a load which is moving almost without any rotation directed towards the positive direction of X_1. It is close to the case studied in paper [1]. It results in a highest deflection ratio of about 1·6 in the X_1 direction. In the X_2 direction there is a small deflection term related to the gyroscopic coupling effect of the rotating shaft. For $k_p = 5$ the load is rotating five times while traversing the shaft. It may be seen that the maximal deflections of the shaft under the moving load become smaller in both directions (less than 0·3).

Figure 9 describes shaft deflection when the value of $\alpha = 1{\cdot}1$. It means higher axial velocity of the load v, and as a result, for each value of k_p also higher rotational speed of the load. It may be observed in Figure 9 that for all cases $U/U_s < 1$.

It should be noticed that in the case of a leading screw, the load pitch length (l_p) is equal to the screw pitch and therefore it is a single-degree-of-freedom system. In practice the pitch is much smaller than the shaft length, which means for $k_p > 10$, $U/U_s \ll 1$. It means that there is a small deflection (and stress) of the shaft and when the load rotates it is highly constrained to a small pitch length. This phenomenon may be explained by the "averaging" effect due to the "dense" rotation of the load. Figure 10 shows results of shaft deflections for $\alpha = 0{\cdot}5$ and for $k_p = 20$. Maximal values of the deflections in both directions are less than 0·02.

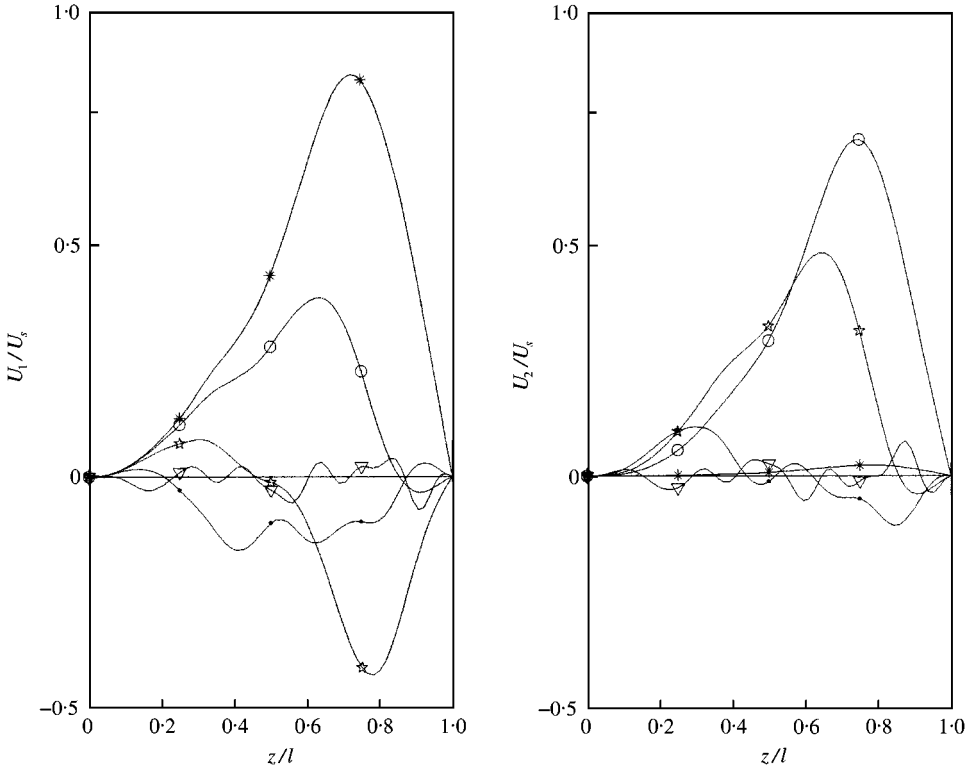

Figure 9. Dynamic deflections of a rotating shaft under moving and rotating load ($\alpha = 1{\cdot}1$; **, $k_p = 0{\cdot}01$; ○, $k_p = 0{\cdot}5$; ☆, $k_p = 1$; ●, $k_p = 2$; ▽, $k_p = 5$).

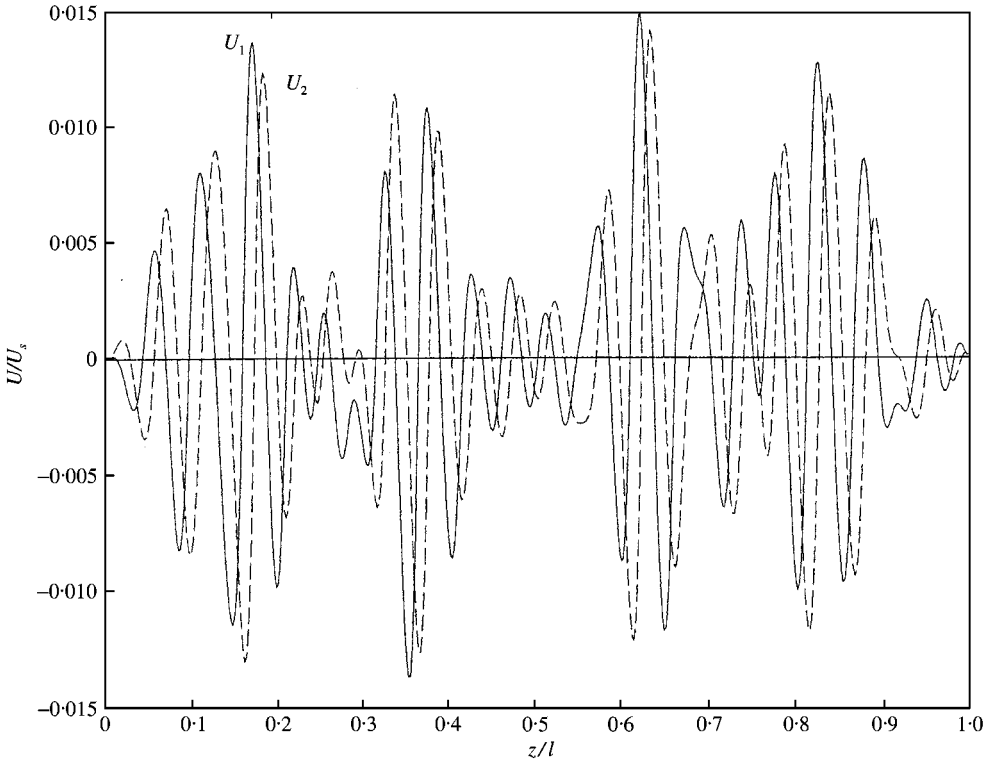

Figure 10. Dynamic deflections of a rotating shaft under moving and rotating load ($k_p = 20$, $\alpha = 0{\cdot}5$).

4.2. EXAMPLE 2—DYNAMIC DEFLECTION AT MID-SPAN OF A STATIONARY SHAFT SUBJECT TO AN AXIALLY MOVING AND ROTATING LOAD

In this example the behaviour of a stationary shaft subject to axially moving and rotating load that may be described as "helical" motion of the load is studied. The study may represent several types of linear bearings. The numerical values of the material and the length of the shaft are as in Table 1. In order to compare the dynamic response of a rotating and non-rotating load; the deflection at mid-span is studied. Figures 11–13 presents the results of the dynamic deflection at mid-span of the shaft at the time interval $t = l/v$, for different values of load speed parameter α. For a non-rotating load ($k_p = 0$), which is only axially moving along the shaft, the results are similar to those presented in reference [4].

Figure 11 is plotted for load speed $\alpha = 0{\cdot}5$. It is observed that the dynamic deflection amplification is significant in both the U_1 and U_2 directions for values below $k_p = 1$ or as long as the load rotates less than one full rotation while traversing the shaft length. As k_p increases the deflection of the shaft is decreasing in both directions. For $k_p = 5$ the maximum dynamic deflection at mid-span is only $0{\cdot}1U_s$, or 10% of the static deflection of a simply supported beam subject to a load at mid-span location.

Figure 12 present results for higher load speed, $\alpha = 1$. Here, as expected, the dynamic amplification is lower than for $\alpha = 0{\cdot}5$. Figure 6 shows that at the initial point ($l = 0$), the load is pointing in the U_1 direction. This initial position of the load of course affects the calculated deflection components in both the U_1 and U_2 directions. To clarify this point the curves for $k_p = 0{\cdot}5$ in Figure 12 will be examined. In this case the load rotates only 180°

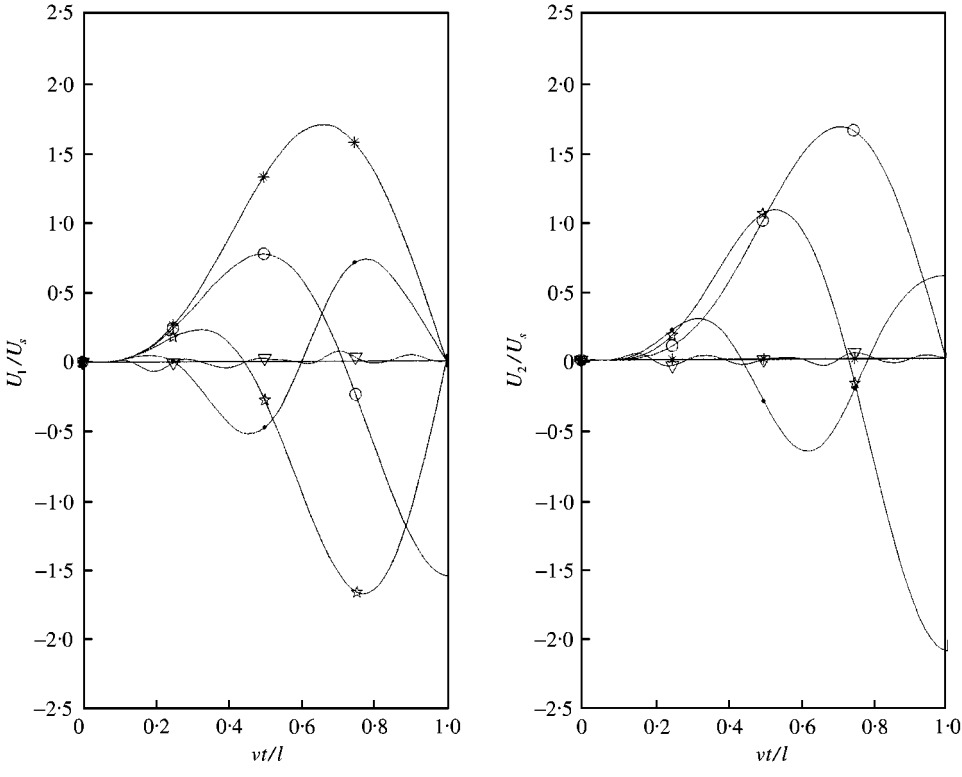

Figure 11. Dynamic deflection at mid-span of stationary shaft subject to a moving and rotating load $U(l/2, t)/U_s$, for load speed $\alpha = 0{\cdot}5$ ($\alpha = 0{\cdot}5$; $*$, $k_p = 0$; $\bigcirc$, $k_p = 0{\cdot}5$; $\star$, $k_p = 1$; $\bullet$, $k_p = 2$; $\bigtriangledown$, $k_p = 5$).

while traversing the length of the shaft. Therefore, when the load reaches mid-span location, it is pointing in the U_2 direction. It explains why the maximum value of U_2/U_s is about 1·3, while in the other direction the value of U_1/U_s is only 0·45.

Figure 13 presents results for a load speed of $\alpha = 2$. Due to the high axial speed of the load, all dynamic deflections at mid-span become smaller than the static deflection at mid-span $U_1/U_s < 1$. As the values of k_p increase, the dynamic response of the shaft decreases.

The dynamic deflections of an axially moving, non-rotating load, on a stationary shaft are only in the U_1 direction, in the plane of its motion. The rotation of the moving load on a stationary shaft creates deflections in both the U_1 and U_2 directions. The dynamic deflections of an axially moving, non-rotating load, on a rotating shaft have components both in the U_1 and U_2 directions, due to the gyroscopic effect, as shown in example 1.

5. SUMMARY AND CONCLUSION

The paper presents the dynamic response of a rotating shaft with simply supported boundary conditions subject to moving and rotating load. In a previous paper [1], the effects of various parameters of a rotating shaft subject to an axially moving load were studied. The general solution shown here enables the effect of the combined axial and

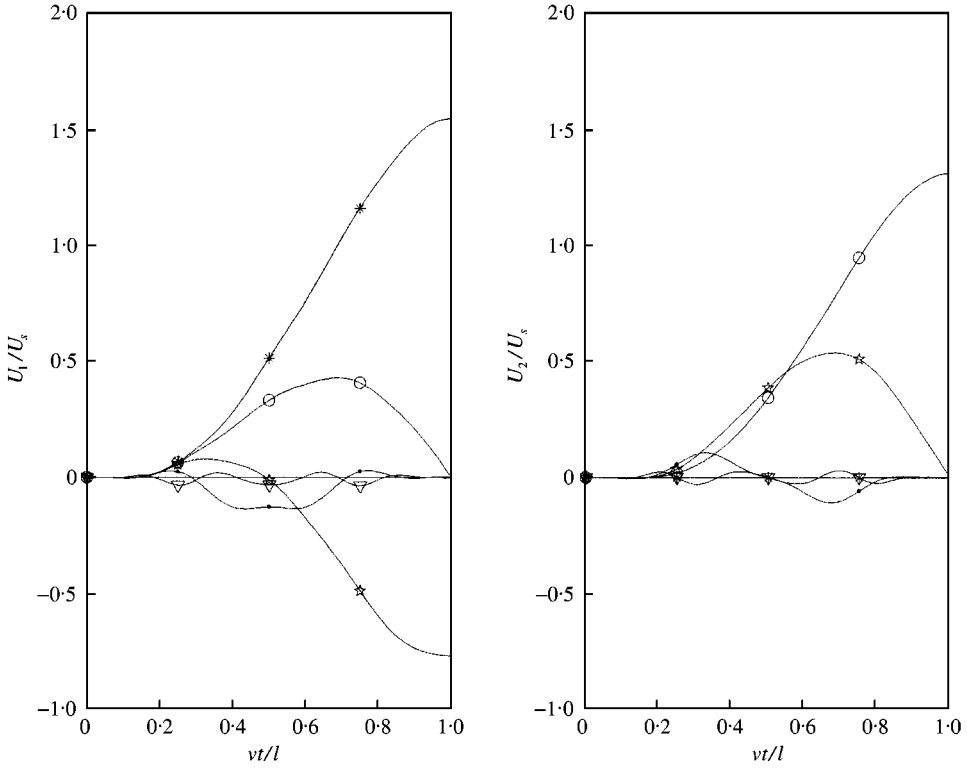

Figure 12. Dynamic deflection at mid-span of stationary shaft subject to a moving and rotating load $U(l/2, t)/U_s$, for load speed $\alpha = 1{\cdot}0$ ($\alpha = 1{\cdot}0$; $*$, $k_p = 0$; $\bigcirc$, $k_p = 0{\cdot}5$; $\star$, $k_p = 1$; $\bullet$, $k_p = 2$; $\bigtriangledown$, $k_p = 5$).

rotational motion of the load to be studied. The present study may be significant in the dynamic analysis of future high-speed and high-precision linear bearings and other mechanical elements. Most papers shown in the references mentioned only future high-speed metal cutting as the motivation for their study.

Based on the investigation presented in the paper it can be concluded that:

1. The dynamic response of a rotating shaft subject to an axially moving and rotating load represents a family of dynamic problems, which are related to future high-speed and high-accuracy mechanical elements. The ability to analyze analytically a three-degrees-of-freedom motion (Ω, v, p) may apply to some other high-speed mechanism design in the future.
2. The dynamic deflection of a rotating shaft which is subject to the prescribed loads has components in both directions (U_1 and U_2) due to the rotating load and due to the gyroscopic coupling.
3. For values of k_p less than one, i.e., when the load is rotating slowly while moving quickly in the axial direction, there is significant dynamic deflection (and stress) amplification of the shaft up to 60% when $k_p = 0{\cdot}01$ and $\alpha = 0{\cdot}5$. For the same value of α, if $k_p > 2$, i.e., the load is making at least two rotations while traversing the shaft, there is an attenuation of the deflection.
4. The deflection components of the shaft U_1 and U_2 decrease as the load pitch length l_p decreases (equivalent to increasing values of k_p).

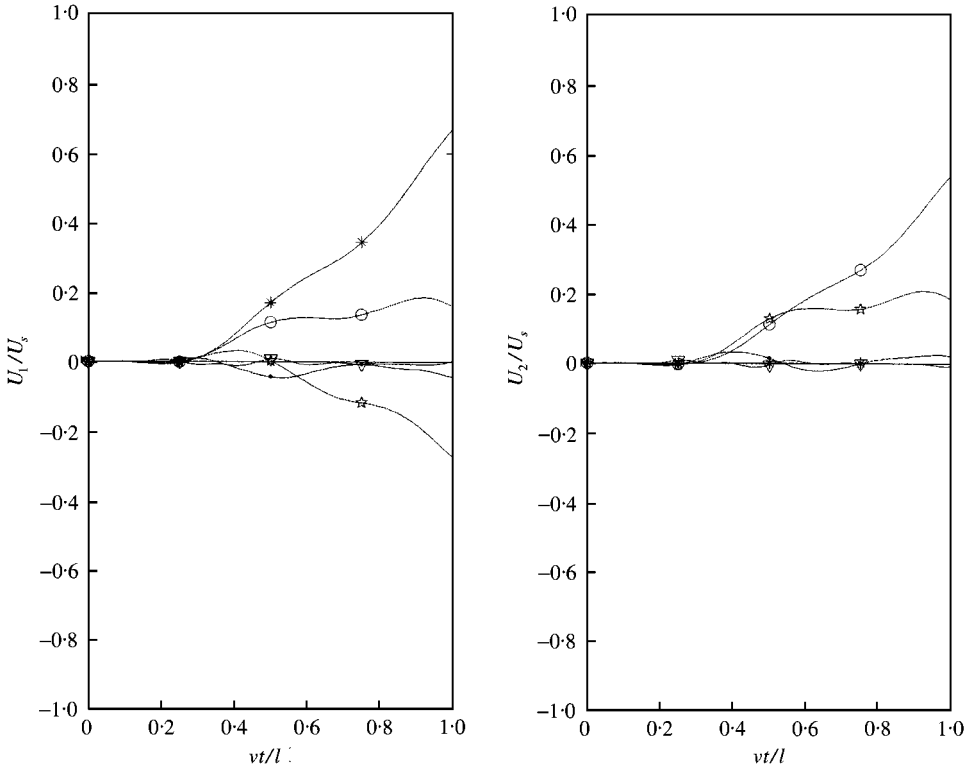

Figure 13. Dynamic deflection at mid-span of stationary shaft subject to a moving and rotating load $U(l/2, t)/U_s$, for load speed $\alpha = 2{\cdot}0$ ($\alpha = 2{\cdot}0$; $*$, $k_p = 0$; $\bigcirc$, $k_p = 0{\cdot}5$; $\star$, $k_p = 1$; $\bullet$, $k_p = 2$; $\bigtriangledown$, $k_p = 5$).

5. The dynamic deflections of an axially moving, non-rotating load, on a stationary shaft are only in the U_1 direction, in the plane of load motion. The rotation of the moving load on a stationary shaft creates deflections in both the U_1 and U_2 directions.

REFERENCES

1. R. KATZ, C. W. LEE, A. G. ULSOY and R. A. SCOTT 1988 *Journal of Sound and Vibration* **122**(1), 131–148. The dynamic response of a rotating shaft subject to a moving load.
2. F. M. DIMENTBERG 1961 *Flexural Vibration of Rotating Shafts*. London: Butterworth.
3. R. L. ESHLEMAN and R. A. EUBANKS 1969 *American Society of Mechanical Engineers Journal of Applied Mechanics* **15**, 1180–1188. On the critical speeds of a continuous rotor.
4. L. FRYBA 1972 *Vibration of Solids and Structures under Moving Loads*. Groningen, The Netherlands: Noordhoff.
5. C. W. LEE, R. KATZ, A. G. ULSOY and R. A. SCOTT 1988 *Journal of Sound and Vibration* **122**, 119–130. Modal analysis of a distributed parameter rotating shaft.
6. A. ARGENTO and R. A. SCOTT 1992 *Journal of Sound and Vibration* **157**, 221–231. Dynamic response of a rotating beam subjected to an accelerating distributed surface load.
7. A. ARGENTO, H. L. MORENO and R. A. SCOTT 1994 *Journal of Vibration and Acoustics* **116**, 397–403. Accelerating load on a rotating Rayleigh beam.
8. S. C. HUANG and J. S. CHEN 1990 *Journal of the Chinese Society of Mechanical Engineering* **11**, 63–73. Dynamic response of orthotropic beams subjected to moving harmonic forces.
9. S. C. HUANG and B. S. HSU 1990 *Journal of Sound and Vibration* **136**, 215–228. Resonant phenomena of a rotating cylindrical shell subjected to a harmonic moving load.

10. J. W. Z. ZU and R. P. S. HAN 1994 *Journal of Applied Mechanics* **61**, 152–160. Dynamic response of spinning Timoshenko beam with general boundary conditions and subjected to a moving load.
11. C. W. LEE 1993 *Vibration Analysis of Rotors*. The Netherlands: Kluwer Academic Publisher.
12. H. P. LEE 1995 *Journal of Sound and Vibration* **181**, 169–177. Dynamic response of rotating Timoshenko shaft subject to axial forces and moving load.
13. S. CHOI 1992 *Ph.D. Dissertation, University of Michigan, Ann Arbor*. Vibration localization in rotating shafts.